

Phase Relationships of the Lithium Halide Spinel $\text{Li}_2\text{MCl}_4\text{-Li}_2\text{MBr}_4$ with $M = \text{Mn, Fe, Cd}$

H. D. LUTZ, W. SCHMIDT, AND H. HAEUSELER

*Laboratorium für Anorganische Chemie der Universität Siegen,
Adolf-Reichwein-Strasse, D 5900 Siegen, Federal Republic of Germany*

Received April 24, 1984; in revised form July 9, 1984

The sections $\text{Li}_2\text{MCl}_{4-4x}\text{Br}_{4x}$ of the quaternary systems $\text{LiCl-LiBr-MCl}_2\text{-MBr}_2$ with $M = \text{Mn, Cd, and Fe}$ were studied by high-temperature X-ray diffraction patterns and DTA and DSC measurements. In the quasibinary lithium manganese halide system complete series of solid solutions exist between the inverse spinels Li_2MnCl_4 and Li_2MnBr_4 . Li_2MnBr_4 and solid solutions with $x > 0.54$ undergo phase transitions to tetragonal spinels at lower temperatures. In the nonquasibinary system with $M = \text{Cd}$, only at temperatures near 400°C a complete series of mixed crystals is formed. At lower temperatures the system is mainly two-phase with rock salt-type $\text{Li}_{1-y}\text{Cd}_{0.5y}\text{Cl}_{1-x}\text{Br}_x$ and cadmium chloride-type $\text{Cd}_{1-y}\text{Li}_{2y}\text{Cl}_{2-2x}\text{Br}_{2x}$ solid solutions in equilibrium. The lithium iron halide system is similar to that of cadmium, but spinel-type Li_2FeBr_4 does not exist at any temperature. The manganese and cadmium halide spinels and spinel solid solutions undergo phase transitions to NaCl defect structures at elevated temperatures. © 1985 Academic Press, Inc.

Introduction

The lithium chloride spinels Li_2MCl_4 with $M = \text{Mg, Mn, Fe, and Cd}$ (1, 2) were found to be fast lithium ion conductors (3-6). Recent studies (7, 8) showed that the lithium bromide spinels Li_2MnBr_4 and Li_2CdBr_4 (9) possess a likewise large lithium ion conductivity. In this paper, we report on the phase diagrams of the lithium halide spinel systems and the preparation of mixed chloride bromide lithium spinels $\text{Li}_2\text{MCl}_{4-4x}\text{Br}_{4x}$ ($M = \text{Mn, Fe, Cd}$).

The phase diagrams under discussion are not known so far. The ternary spinels, first reported in 1975 (1) and 1981 (9), undergo phase transitions to NaCl defect structures at elevated temperatures with highly disordered metal sublattices compared to the

spinel structure (2, 9). Furthermore, the bromide spinels are not stable at room temperature (9) (contrary to the corresponding chlorides). Cubic Li_2MnBr_4 is distorted to a tetragonal modification. Li_2CdBr_4 is decomposed to a rock salt-type $\text{Li}_{1-x}\text{Cd}_{0.5x}\text{Br}$ and a cadmium chloride-type $\text{Cd}_{1-x}\text{Li}_{2x}\text{Br}_2$ solid solution.

Experimental Methods

The starting materials were the binary halides $\text{LiCl, LiBr, MnCl}_2, \text{CdCl}_2$ (all from Merck), and FeBr_2 (Ventron). FeCl_2 was obtained by dehydration of $\text{FeCl}_2 \cdot 4\text{H}_2\text{O}$ under vacuum at $300\text{-}500^\circ\text{C}$ (10), MnBr_2 and CdBr_2 by conversion of the acetate hydrates with acetyl bromide in toluol or *n*-hexane (11). The halides of the bivalent

metals were purified before use by crystallization from the melt (technique of Bridgman) (12). LiCl and LiBr were of analytical quality.

The ternary and quaternary halides were prepared by fusing the binary compounds in evacuated sealed borosilicate glass ampoules. Details are given elsewhere (2, 4, 7). The chlorides and bromides under investigation are extremely hygroscopic and, in the case of the iron compounds, sensitive to oxygen. They must be handled under a dry-argon atmosphere.

The obtained compounds were characterized with X-ray Guinier powder technique (Huber Guinier 600 system), using $\text{CuK}\alpha_1$ radiation. The unit cell dimensions of the halide spinels and spinel solid solu-

tions were calculated by least-squares methods. Quartz was used as an internal standard (SiO_2 , $a_0 = 491.36$ and $c_0 = 540.54$ pm). High-temperature X-ray diffraction patterns were obtained with an Enraf-Nonius Guinier Simon FR 533 camera, using $\text{CuK}\alpha_1$ radiation. Sealed quartz capillaries, which were protected from reaction with the halide at elevated temperatures by a graphite layer (2), were taken for sample holders.

The DSC (differential scanning calorimetry) and the DTA (differential thermal analysis) measurements were made in an argon stream and in evacuated sealed borosilicate glass tubes with the Perkin-Elmer differential scanning calorimeter DSC2 and the thermoanalyzer Linseis L62, respectively.

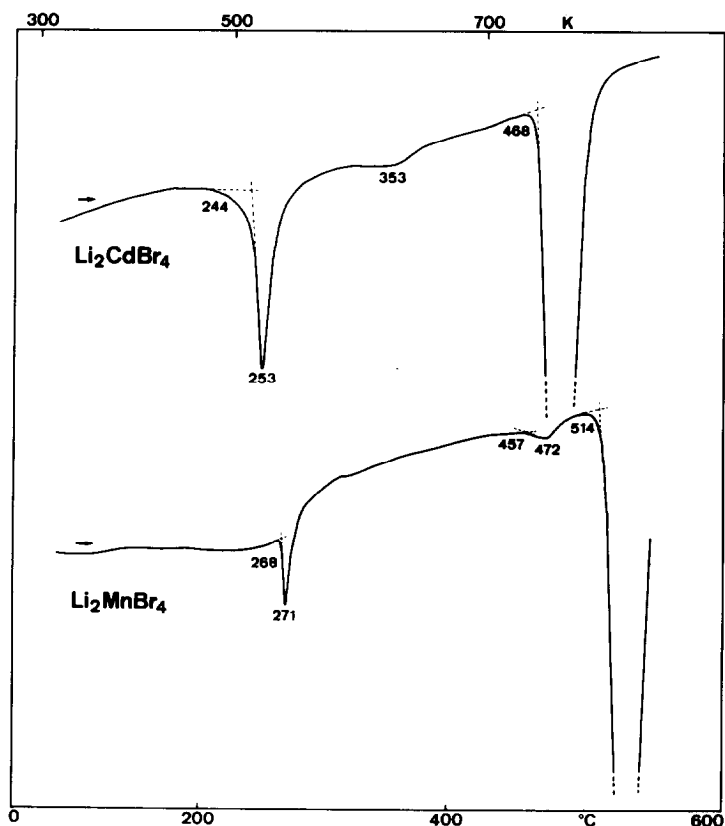


FIG. 1. DTA diagrams of Li_2MnBr_4 and Li_2CdBr_4 (sealed evacuated glass tubes, heating rate 5°C min^{-1}), giving temperature (phase transitions and melting points) intersections and peak maxima.

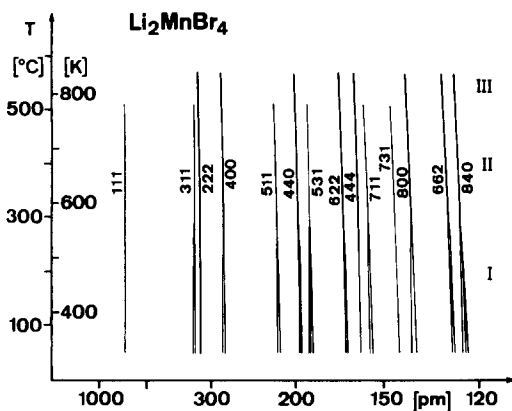


FIG. 2. High-temperature X-ray diffraction pattern of Li_2MnBr_4 : I, tetragonal distorted spinel; II, cubic spinel; III, rock salt defect structure.

The heating rates were 5°C min^{-1} . The reference was Al_2O_3 .

Results

1. The Quasibinary System $\text{Li}_2\text{MnCl}_4\text{--Li}_2\text{MnBr}_4$

Figure 1 shows the DTA results of the ternary Li_2MnBr_4 (for Li_2MnCl_4 see (2)). The endothermic peaks at 268 and 457°C (intersections) show the tetragonal to cubic and the spinel to defect rock salt-phase transitions. A high-temperature X-ray diffraction pattern of Li_2MnBr_4 is given in Fig. 2. The phase diagram of the system $\text{Li}_2\text{MnCl}_{4-4x}\text{Br}_{4x}$ is shown in Fig. 3. Complete series of solid solutions are formed between the chloride and the bromide spinel. The phase transition to the tetragonal low-temperature modification found for the bromide (9) can be observed down to $x = 0.54$. The lattice constants of the spinel solid solutions obey Vegard's law (see Fig. 4). From Fig. 4 it is further shown that the a and b axes of the tetragonal $\text{Li}_2\text{MnCl}_{4-4x}\text{Br}_{4x}$ -mixed crystals are shortened compared to the c axis, which obviously resembles the lattice constant of the undistorted cubic spinel. The Guinier patterns of samples with $x = 0.5\text{--}0.6$, however, show relatively

diffuse reflections. The tetragonal distortion, i.e., the c/a ratio, of the Br-rich solid solutions conspicuously is largest near the phase boundary to the cubic spinel.

2. The System $\text{Li}_2\text{CdCl}_{4-4x}\text{Br}_{4x}$

Unlike the manganese system, a complete series of solid solutions between Li_2CdCl_4 and Li_2CdBr_4 is only formed in a small temperature region near 400°C . At lower temperatures, the mixed crystals decompose to rock salt-type $\text{Li}_{1-y}\text{Cd}_{0.5y}\text{Cl}_{1-x}\text{Br}_x$ and cadmium chloride type $\text{Cd}_{1-y}\text{Li}_{2y}\text{Cl}_{2-2x}\text{Br}_{2x}$ solid solutions. At ambient temperature less than 5% bromide can be incorporated into the chloride spinel. The unit cell dimension of the bromide-richest spinel is 1068(1) pm compared to 1063.5(9) pm of Li_2CdCl_4 (2). The DTA diagrams and the high-temperature X-ray diffraction patterns of the ternary Li_2CdBr_4 (see Figs. 1 and 5) show the decomposition of the bromide spinel to the $\text{Li}_{1-y}\text{Cd}_{0.5y}\text{Br}$ and $\text{Cd}_{1-y}\text{Li}_{2y}\text{Br}_2$

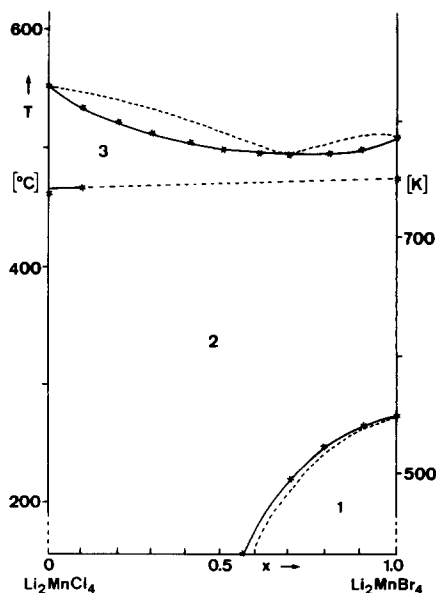


FIG. 3. Phase diagram of the quasibinary system $\text{Li}_2\text{MnCl}_4\text{--Li}_2\text{MnBr}_4$ ($\text{Li}_2\text{MnCl}_{4-4x}\text{Br}_{4x}$): (1) tetragonal distorted spinel; (2) cubic spinel; (3) rock salt defect structure; DTA peaks (intersection, see Fig. 1).

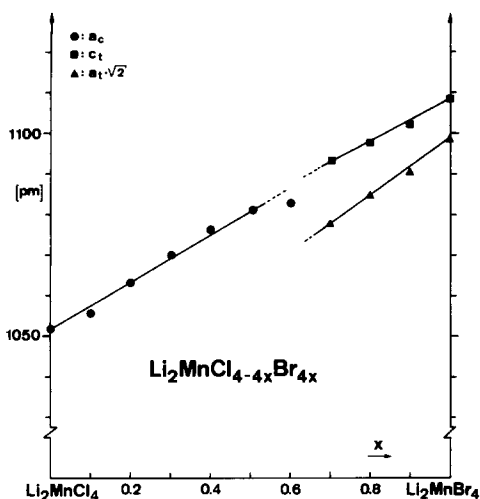


FIG. 4. Lattice constants of $\text{Li}_2\text{MnCl}_{4-4x}\text{Br}_{4x}$ spinel-type solid solutions, slowly cooled to room temperature: a_c , lattice constant of the cubic spinel; a_t and c_t , lattice constants of tetragonal distorted spinel; $a_t \cdot \sqrt{2}$ is plotted for better comparison with a_c .

mixed crystals below 244°C (intersection) and the order–disorder transition to the defect rock salt structure above 353°C .

3. The System Li_2FeCl_4 – Li_2FeBr_4

The system $\text{Li}_2\text{FeCl}_{4-4x}\text{Br}_{4x}$ is similar to the cadmium halide system, discussed above, however, with two exceptions. The chloride spinel does not undergo a phase

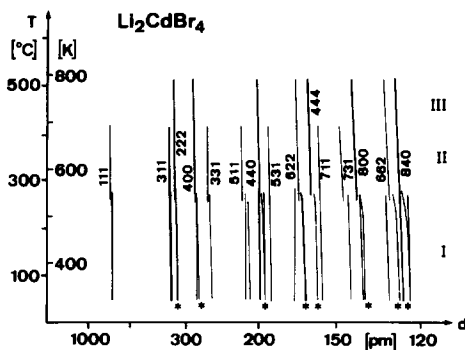


FIG. 5. High-temperature X-ray diffraction pattern of Li_2CdBr_4 : I, two-phase, $\text{Li}_{1-y}\text{Cd}_{0.5y}\text{Br}$ (reflections marked by asterisks) and $\text{Cd}_{1-y}\text{Li}_{2y}\text{Br}_2$; II, spinel; III, NaCl defect structure.

transition to a defect rock salt structure (2) and a spinel-type Li_2FeBr_4 does not exist at any temperature. At ambient temperatures spinel-type $\text{Li}_2\text{FeCl}_{4-4x}\text{Br}_{4x}$ -mixed crystals exist up to $x = 0.15$. For details see Ref. (7). Furthermore, $\text{Li}_2\text{Mn}_{1-x}\text{Fe}_x\text{Br}_4$ solid solutions have been prepared.

Discussion and Conclusion

The spinel-type halide solid solutions are likewise fast lithium ion conductors as the ternary chloride and bromide spinels (7, 8). This is due to the high mobility and disorder of the lithium ions. For the same reason, reaction and phase transition rates of the halide spinels are very large (contrary to oxide and chalcide spinels), and, hence, all high-temperature modifications, i.e., cubic Li_2MnBr_4 , Li_2CdBr_4 , and the defect rock salt-type compounds, cannot be quenched to ambient temperature.

The phase transitions to the defect rock salt structures are obviously of order–disorder type, in the course of which the lithium ions are disordered at lower temperatures than the divalent ions (2, 7, 8). The latter is shown by the disappearance of the spinel (superstructure) reflections in the high-temperature X-ray diffraction patterns (see Figs. 2 and 5). Less intelligible is the nature of the tetragonal to cubic-phase transition of Li_2MnBr_4 spinel, which can also be performed with monocrystals.

The bromide spinels are obviously less stable than the chloride spinels. This behavior is presumably due to the larger polarizability of bromide ions, which favors layer structures.

Acknowledgments

The authors thank cand. chem. P. Kuske for experimental help and the Deutsche Forschungsgemeinschaft and the Fonds der Chemischen Industrie for financial support.

References

1. C. J. J. VAN LOON AND J. DE JONG, *Acta Crystallogr. Sect. B* **31**, 2549 (1975).
2. H. D. LUTZ, W. SCHMIDT, AND H. HAEUSELER, *Z. Anorg. Allg. Chem.* **453**, 121 (1979).
3. H. D. LUTZ, W. SCHMIDT, AND H. HAEUSELER, "Proceedings, 9th International Symposium on the Reactivity of Solids, Cracow, Poland, Sept. 1-6, 1980"; *Mater. Sci. Monogr.* **10**, 200 (1982).
4. H. D. LUTZ, W. SCHMIDT, AND H. HAEUSELER, *J. Phys. Chem. Solids* **42**, 287 (1981).
5. R. KANNO, Y. TAKEDA, AND O. YAMAMOTO, *Mater. Res. Bull.* **16**, 999 (1981).
6. J. SPECTOR, G. VILLENEUVE, L. HANEBALI, AND C. CROS, *Mater. Lett.* **1**, 43 (1982).
7. W. SCHMIDT, dissertation, University of Siegen (1983).
8. W. SCHMIDT AND H. D. LUTZ, *Ber. Bunsenges. Phys. Chem.* **88**, 720 (1984).
9. H. D. LUTZ, W. SCHMIDT, AND H. HAEUSELER, *Naturwissenschaften* **68**, 328 (1981).
10. G. GARTON AND P. J. WALKER, *J. Cryst. Growth* **33**, 331 (1976).
11. G. W. WATT, P. S. GENTILE, AND E. P. HELVENSTON, *J. Amer. Chem. Soc.* **77**, 2752 (1955).
12. S. LEGRAND, *J. Cryst. Growth* **35**, 208 (1976).